Frontiers of Information Technology & Electronic Engineering
www.jzus.zju.edu.cn; engineering.cae.cn; www.springerlink.com
ISSN 2095-9184 (print); ISSN 2095-9230 (online)
E-mail: jzus@zju.edu.cn

Swarm intelligent computing of electric eel foraging heuristics for fractional Hammerstein autoregressive exogenous noise model identification#

Faisal ALTAF[1], Ching-Lung CHANG[2], Naveed Ishtiaq CHAUDHARY[†‡3], Taimoor Ali KHAN[4], Zeshan Aslam KHAN[4,5], Chi-Min SHU[6], Muhammad Asif Zahoor RAJA[3]

[1]*Graduate School of Engineering Science and Technology, Yunlin University of Science and Technology, Yunlin 64002, Taiwan, China*
[2]*Department of Computer Science and Information Engineering, Yunlin University of Science and Technology, Yunlin 64002, Taiwan, China*
[3]*Future Technology Research Center, Yunlin University of Science and Technology, Yunlin 64002, Taiwan, China*
[4]*International Graduate School of Artificial Intelligence, Yunlin University of Science and Technology, Yunlin 64002, Taiwan, China*
[5]*Department of Electrical and Computer Engineering, International Islamic University, Islamabad 44000, Pakistan*
[6]*Department of Safety, Health and Environmental Engineering, Yunlin University of Science and Technology, Yunlin 64002, Taiwan, China*
[†]E-mail: chaudni@yuntech.edu.tw

Received Aug. 20, 2024; Revision accepted Dec. 1, 2024; Crosschecked Oct. 22, 2025

Abstract: Fractional calculus is considered a useful tool for gaining deeper insights into systems with memory effects or history. Fractional-order modeling of nonlinear systems may increase the stiffness and complexity of the system, but also provides better insights. This study introduces a swarm intelligence-based parameter estimation of the fractional Hammerstein autoregressive exogenous noise (fractional-HARX) model. The Grünwald–Letnikov finite difference formula is used to develop the fractional-HARX model from the standard HARX model. This study presents the design of a swarm intelligence-based electric eel foraging optimization algorithm (EEFOA) for parameter estimation of the fractional-HARX model under multiple noise scenarios for second- and third-order polynomial type nonlinearity. The key-term separation principle is also incorporated in the system model to reduce the occurrence of redundant parameters due to cross-product terms in the information vector. The designed methodology is examined, and the superiority of EEFOA is endorsed in terms of convergence, robustness, stiff parameter estimation, and deviation from the mean point in comparison with state-of-the-art optimization heuristics such as the whale optimization algorithm, the African vulture optimization algorithm, Harris hawk's optimizer, and the reptile search algorithm. The statistical significance of the EEFOA for the estimation of fractional-HARX models is also established using statistical indices of best, mean, and worst fitness values along with standard deviation for multiple noise scenarios.

Key words: Fractional calculus; Nonlinear systems; Electric eel foraging; Intelligent computing
https://doi.org/10.1631/FITEE.2400730 **CLC number:** TP271

1 Introduction

Fractional calculus has been utilized to simulate various mathematical and physical processes across multiple domains (Sweis et al., 2023; Frikh and Boutasseta, 2024; Megherbi et al., 2024), including digital image processing (Gamini and Kumar, 2023), engineering (Partohaghighi et al., 2024), biomedicine

‡ Corresponding author
# Electronic supplementary materials: The online version of this article (https://doi.org/10.1631/FITEE.2400730) contains supplementary materials, which are available to authorized users
ORCID: Faisal ALTAF, https://orcid.org/0009-0007-7621-5875; Naveed Ishtiaq CHAUDHARY, https://orcid.org/0000-0002-9568-3216

(Ionescu et al., 2017; Mukhtar et al., 2024), control systems (Li ZQ et al., 2023; Zhang XF et al., 2023), power systems (Padhi et al., 2023; Sowa et al., 2023), signal processing (Machado and Lopes, 2015; Karaca, 2023), electrical circuits (Kausar et al., 2025), and stress detection (Šapina et al., 2020). Additionally, its applications include lithium–ion batteries (Wang SW et al., 2024), fractional neural networks (Li S et al., 2023), the modeling of COVID-19 transmission (Mehmood N et al., 2023), hybrid viscous nanofluids (Ali et al., 2021), and nuclear reactors (Vyawahare and Nataraj, 2013). The unique capabilities of fractional calculus are beneficial for enhanced mathematical modeling and gaining better insights into systems. The Hammerstein model, which includes the combination of static nonlinear and dynamic linear blocks, has been used in the modeling of various nonlinear systems (Li F et al., 2023a, 2023c; Zhang MG et al., 2024). The structure allows simplified and powerful representation of complex systems, making it a valuable tool for real-world applications. The identification of the Hammerstein nonlinear system is considered a challenging task due to its stiffness and complexity (Li F et al., 2023b, 2024; Hu et al., 2024; Liu et al., 2024). The employment of fractional calculus is also involved in Hammerstein or input nonlinear systems for improved insight into the complex system (Malik MF et al., 2023; Khan et al., 2024a, 2024b; Altaf et al., 2025).

Metaheuristics have proven to be highly efficient in solving complex problems in diversified fields (Ye et al., 2023), for instance, identifying electro-hydraulic actuator systems (Mehmood K et al., 2024), biomedical engineering (Han et al., 2023), feature selection (Fang and Liang, 2023), and microelectronics and nanophotonics (Jakšić et al., 2023). In addition, applications of swarm intelligence-based algorithms can be found in hydraulic performance prediction (Rahmanshahi et al., 2024), supply chain management (Ala et al., 2024), estimation of multi-frequency sinusoidal signaling (Malik NA et al., 2024), big data predictive modeling (El-Hasnony et al., 2020), data mining (Mathi and Baburaj, 2022), spam detection (Tubishat et al., 2023), economic emission dispatching (Dong et al., 2023), machine learning (Abdollahzadeh et al., 2024), and cancer diagnosis (González-Patiño et al., 2019). These investigations motivate the authors to delve into the newly proposed bio-inspired algorithm known as the electric eel foraging optimization algorithm (EEFOA). EEFOA was proposed by Zhao WG et al. (2024). EEFOA is influenced by the sophisticated collective foraging activities displayed by electric eels in their natural habitat. The mathematical model is based on searching behavior, including interaction, resting, hunting, and migration. The proposed optimization technique allows exploration and exploitation at the same stage of optimization. Moreover, the energy factor is devised to regulate the shift from global search to local search while maintaining an optimal balance. The efficacy of EEFOA is validated through comparison with 12 other algorithms using 23 test functions from the Congress on Evolutionary Computation (CEC) 2011 and CEC 2017 test packages. The test results demonstrate the overwhelmingly superior performance of EEFOA in comparison with other algorithms. The effectiveness of EEFOA is thoroughly evaluated through the examination of 10 engineering challenges, including sluice opening control management in a hydro-power facility under disaster tripping situations.

The results indicate the superior performance and great potential of EEFOA in addressing various complex real-world challenges. EEFOA's unique problem-solving capabilities motivate the authors to exploit it for a given problem. The primary objective of this research is to investigate the use of bio-inspired EEFOA for stiff parameter estimation of the fractional Hammerstein autoregressive exogenous noise (fractional-HARX) model with key-term separation. EEFOA is investigated for multiple noise variations in comparison with the state-of-the-art in optimization heuristics such as the whale optimization algorithm (WOA) (Mirjalili and Lewis, 2016), the African vulture optimization algorithm (AVOA) (Abdollahzadeh et al., 2021), Harris hawk's optimizer algorithm (HOA) (Heidari et al., 2019), and the reptile search algorithm (RSA) (Abualigah et al., 2022). The key-term separation principle is incorporated to reduce the occurrence of redundant parameters due to cross-product terms in the information vector of the system (Wang DQ, 2024). The innovative contributions of the scheme are succinctly outlined as follows:

1. The swarm intelligence-based computing of EEFOA is efficaciously exploited for parameter estimation in fractional Hammerstein autoregressive systems with exogenous noise.

2. The key-term separation principle is incorporated to reduce the complexity by avoiding the redundant parameters that occur due to cross-product terms in the information vector.

3. The value of the devised optimization technique is confirmed by way of experimentation in several noisy environments considered in the fractional-HARX model with multiple orders of nonlinearity.

4. The efficacy of the proposed EEFOA is endorsed through its robust, accurate, convergent, and stable performance in comparison with state-of-the-art optimization heuristics.

2 Fractional-HARX model

The fractional-HARX model is represented by a block structure diagram in Fig. 1, where $m(t)$ represents the input, $c(t)$ represents the output, and the exogenous noise is represented by $u(t)$. The mathematical expression is given in Eq. (1):

$$c(t)=\frac{J(z)}{K(z)}\bar{m}(t)+\frac{1}{K(z)}u(t), \tag{1}$$

where the polynomials $K(z)$ and $J(z)$ having fractional order γ are given as

$$K(z)=1+k_1(z^{-1})^{\gamma}+k_2(z^{-2})^{\gamma}+\cdots+k_{n_k}(z^{-n_k})^{\gamma}, \tag{2}$$

$$J(z)=j_0+j_1(z^{-1})^{\gamma}+j_2(z^{-2})^{\gamma}+\cdots+j_{n_j}(z^{-n_j})^{\gamma}. \tag{3}$$

The output of the nonlinear block in the model is obtained by applying the nonlinear function f, as expressed below:

$$\bar{m}(t)=f(m(t)), \tag{4}$$

$$f(m(t))=[f_1(m(t)),f_2(m(t)),\cdots,f_{n_r}(m(t))], \tag{5}$$

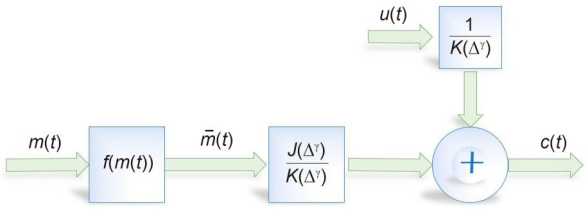

Fig. 1 Fractional-HARX block diagram

$$\begin{aligned}\bar{m}(t)&=r_1m(t)+r_2(m(t))^2+\cdots+r_{n_r}(m(t))^{n_r}\\&=\sum_{j=1}^{n_r}r_jf_j(m(t)).\end{aligned} \tag{6}$$

The significance of fractional-order derivatives lies in their capability to handle differentiation problems of non-integer orders. Multiple mathematical operators defining fractional-order derivatives have been introduced by the research community, such as the Atangana–Baleanu and Caputo–Fabrizio derivatives, the Hilfer fractional derivative, the Liouville–Caputo derivative, the Katugampola fractional derivative, and the Grünwald–Letnikov fractional derivative (GL-FD). Notably, Riemann–Liouville and Caputo exist with varying properties and interpretations. The GL-finite difference operator for $c(t)$ is formulated as (Malik MF et al., 2022)

$$\begin{cases}D^{\gamma}[c(t)]=\dfrac{1}{b^{\gamma}}\displaystyle\sum_{i=0}^{[\gamma]}(-1)^i\binom{\gamma}{i}c(a-ib),\\[2ex]\dbinom{\gamma}{i}=\begin{cases}1, i=0,\\ \dfrac{\gamma(\gamma-1)\ldots(\gamma-i+1)}{i!}, i>0,\end{cases}\end{cases} \tag{7}$$

where $t=ab$, a is the sampling size, b is the total number of samples, and $\lceil\ \rceil$ refers to rounding to the nearest integer for the γ value.

By putting Eqs. (2), (3), and (6) into Eq. (1), Eq. (8) can be obtained:

$$c(t)=-\sum_{i=1}^{n_k}k_iD^{\gamma}[c(t-i)]+\sum_{i=0}^{n_j}j_iD^{\gamma}[\bar{m}(t-i)]+u(t). \tag{8}$$

The key-term separation technique is a valuable tool for system identification, particularly for nonlinear systems like the Hammerstein model. It helps achieve a better parameter estimation by avoiding the estimation of redundant parameters, ultimately leading to a more efficient identification process. Considering $\bar{m}$ a key term and assuming $j_0=1$, we have

$$\begin{aligned}c(t)=&-\sum_{i=1}^{n_k}k_iD^{\gamma}[c(t-i)]+j_0D^{\gamma}[\bar{m}(t)]\\&+\sum_{i=1}^{n_j}j_iD^{\gamma}[\bar{m}(t-i)]+u(t),\end{aligned} \tag{9}$$

$$c(t) = -\sum_{i=1}^{n_k} k_i D^{\gamma}[c(t-i)] + \sum_{i=1}^{n_j} j_i D^{\gamma}[\bar{m}(t-i)] + D^{\gamma}\sum_{i=1}^{n_r} r_i f_i(m(t)) + u(t). \tag{10}$$

The parameters and the corresponding information vectors are expressed as

$$\boldsymbol{\omega}_k(t) = [-D^{\gamma}c(t-1), -D^{\gamma}c(t-2), \cdots, -D^{\gamma}c(t-n_k)]^{\mathrm{T}}, \tag{11}$$

$$\boldsymbol{\omega}_j(t) = [\bar{m}(t-1), \bar{m}(t-2), \cdots, \bar{m}(t-n_j)]^{\mathrm{T}}, \tag{12}$$

$$\boldsymbol{\omega}_r(t) = [f_1(m(t)), f_2(m(t)), \cdots, f_{n_r}(m(t))]^{\mathrm{T}}, \tag{13}$$

$$\boldsymbol{k} = [k_1, k_2, \cdots, k_{n_k}]^{\mathrm{T}}, \tag{14}$$

$$\boldsymbol{j} = [j_1, j_2, \cdots, j_{n_j}]^{\mathrm{T}}, \tag{15}$$

$$\boldsymbol{r} = [r_1, r_2, \cdots, r_{n_r}]^{\mathrm{T}}. \tag{16}$$

At this stage, the key-term-separated fractional-HARX model is given as

$$c(t) = \boldsymbol{\omega}_k^{\mathrm{T}}(t)\boldsymbol{k} + \boldsymbol{\omega}_j^{\mathrm{T}}(t)\boldsymbol{j} + \boldsymbol{\omega}_r^{\mathrm{T}}(t)\boldsymbol{r} + u(t). \tag{17}$$

The corresponding fitness function for the fractional-HARX model in terms of the mean squared error via the difference between $c(t)$ (actual response) and $\hat{c}(t)$ (estimated response) is formulated as

$$\text{Fitness} = \text{mean}\left[\left(c(t) - \hat{c}(t)\right)^2\right]. \tag{18}$$

The estimated response of the fractional-HARX model is given as

$$\hat{c}(t) = \boldsymbol{\omega}_k^{\mathrm{T}}(t)\hat{\boldsymbol{k}} + \boldsymbol{\omega}_j^{\mathrm{T}}(t)\hat{\boldsymbol{j}} + \boldsymbol{\omega}_r^{\mathrm{T}}(t)\hat{\boldsymbol{r}}, \tag{19}$$

and the unknown parameter vector is given as

$$\hat{\boldsymbol{k}} = [\hat{k}_1, \hat{k}_2, \cdots, \hat{k}_{n_k}]^{\mathrm{T}}, \tag{20}$$

$$\hat{\boldsymbol{j}} = [\hat{j}_1, \hat{j}_2, \cdots, \hat{j}_{n_j}]^{\mathrm{T}}, \tag{21}$$

$$\hat{\boldsymbol{r}} = [\hat{r}_1, \hat{r}_2, \cdots, \hat{r}_{n_r}]^{\mathrm{T}}. \tag{22}$$

3 Methodology

EEFOA is a fascinating, newly developed bio-inspired optimization algorithm proposed in 2024, based on the collective search behavior of electric eels in their environment. EEFOA mimics four key foraging behaviors of electric eels, i.e., interaction, resting, hunting, and migration.

These four important behaviors are mathematically modeled for crucial aspects of electric eels. The transition between exploration and exploitation is dynamically controlled by an "energy factor" depending on search progress. However, it is most essential to ensure the adaptability to different problem landscapes. The flowchart of EEFOA is provided in Fig. 2.

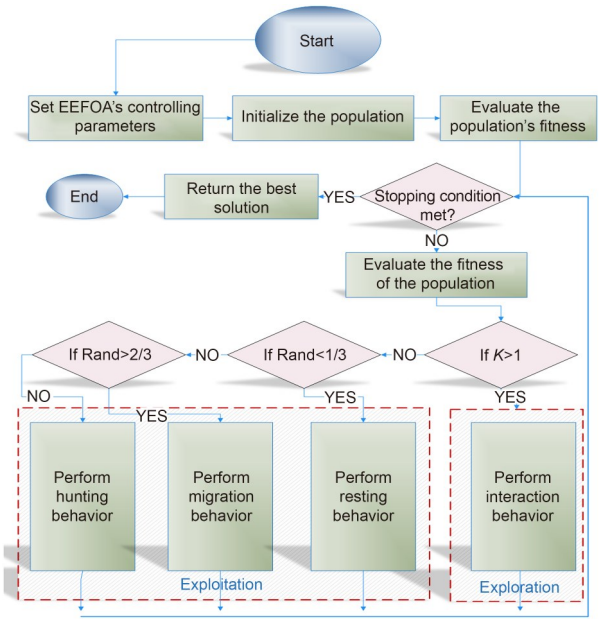

Fig. 2 Flowchart of EEFOA

3.1 Interaction phase

A solution vector containing the optimization variables is represented by an eel in the population. The fitness is computed on the basis of the objective function of the specific problem. In the interaction phase, eels collaborate to explore the search space.

An eel transmits electric pulses and receives signals from other eels. This is known as electrolocation, and is represented by a function, in which the position (distance and direction) of neighboring eels is calculated. However, based on a probability-based

function depending upon fitness and distance, the eels share the best position found. Each individual eel's position is updated depending on its own position established by the information of neighbors and a random term for exploration.

An electric eel within the environment can interact randomly with any other eels within the population by using the regional information (the search space). A churn is a random movement in various directions, and is marked by the interaction of an eel. Mathematically, the churn is modeled as (Zhao WG et al., 2024)

$$\boldsymbol{Q} = n_1 \boldsymbol{W}, \tag{23}$$

$$n_1 \sim N(0,1), \tag{24}$$

$$\boldsymbol{W} = [w_1, w_2, \cdots w_k, \cdots, w_d], \tag{25}$$

$$w(k) = \begin{cases} 1, \text{ if } k = s\{m, \\ 0, \text{ otherwise}, \end{cases} \tag{26}$$

$$s = \text{randperm}(d), \tag{27}$$

$$m = 1, 2, \cdots, \left\lceil \frac{L - t}{L} r_1 (d - 2) + 2 \right\rceil, \tag{28}$$

where L is the maximum number of iterations. Hence, interacting behavior is given as

$$\begin{aligned} &\text{if fitness}(y_j(t)) < \text{fitness}(y_i(t)), \\ &\text{then} \begin{cases} s_i(t+1) = y_j(t) + Q(\bar{y}(t) - y_i(t)), c_1 > 0.5, \\ s_i(t+1) = y_j(t) + Q(y_r(t) - y_i(t)), c_1 \le 0.5, \end{cases} \\ &\text{if fitness}(y_j(t)) \ge \text{fitness}(y_i(t)), \\ &\text{then} \begin{cases} s_i(t+1) = y_i(t) + Q(\bar{y}(t) - y_j(t)), c_2 > 0.5, \\ s_i(t+1) = y_i(t) + Q(y_r(t) - y_j(t)), c_2 \le 0.5, \end{cases} \end{aligned} \tag{29}$$

$$y(t) = \frac{1}{n} \sum_{i=1}^{n} y_i(t), \tag{30}$$

$$y = \text{Low} + r(\text{Up} - \text{Low}), \tag{31}$$

where c_1 and c_2 are the random numbers within (0,1), fitness($y_i(t)$) is the fitness of the i^{th} electric eel's candidate position, y_j is the randomly selected eel's position, Low and Up are the lower and upper boundaries, respectively, and r is a random number within (0,1).

3.2 Resting phase

This phase mimics eels potentially updating their respective positions and taking breaks. During this phase, the transition probability of an eel entering this phase is determined by a random number generator. However, during this phase the eels exploit the neighborhood in their respective search space.

The mathematical expression to define the resting area is given as (Zhao WG et al., 2024)

$$\left\{ X \,|\, X - V(t) | \le \mu_0 \left| V(t) - \boldsymbol{y}_{\text{prey}}(t) \right| \right\}, \tag{32}$$

$$\mu_0 = 2\left(\varepsilon - \varepsilon^{1/L}\right), \tag{33}$$

$$V(t) = \text{Low} + v(t)(\text{Up} - \text{Low}), \tag{34}$$

$$v \left\{ t = \frac{y_{\text{rand}\{n}^{\text{rand}\{d} \{t - \text{Low}^{\text{rand}\{d}}{\text{Up}^{\text{rand}\{d} - \text{Low}^{\text{rand}\{d}}. \tag{35}$$

The variables are defined as follows: $\boldsymbol{y}_{\text{prey}}$ is the position vector, μ_0 is the initial value of the resting area, $\mu_0|V(t) - \boldsymbol{y}_{\text{prey}}(t)|$ is the resting area range, $y_{\text{rand}\{n}^{\text{rand}\{d}$ represents the random position of a randomly selected individual, and $V(t)$ represents a normalized number.

$$R_i(t+1) = V(t) + \mu \left| V(t) - \boldsymbol{y}_{\text{prey}}(t) \right|, \tag{36}$$

$$\mu = \mu_0 \sin(2\pi r_2), \tag{37}$$

where μ is the resting area scale and r_2 is a random number within (0,1).

As the iteration proceeds, the resting area range decreases, enhancing the exploitation. As the resting area is determined, the eels move towards it by updating their positions. This behavior can be mathematically expressed as

$$\begin{aligned} s_i(t+1) = {} & R_i(t+1) \\ & + n_2 (R_i(t+1) \text{round}(\text{rand}) y_i(t)), \end{aligned} \tag{38}$$

$$n_2 \sim N(0,1), \tag{39}$$

where round means to round off the random value.

3.3 Hunting phase

Instead of directly hunting the prey selected in the search space, the eels make a large circle around the prey and start peer-to-peer communication by transmitting low voltage signals. As the eels' communication increases, the circle shrinks and the eels drive the prey towards the shallow end. However, after being frightened, the prey moves into the electrically charged circle, and updates its respective position, that is, its position with respect to its current position in the hunting space. Mathematically, the hunting area is expressed as

$$\left\{X \middle| X - \boldsymbol{y}_{\text{prey}}(t) \middle| \leq \eta_0 \middle| \bar{\boldsymbol{y}}(t) - \boldsymbol{y}_{\text{prey}}(t) \middle| \right\}, \quad (40)$$

$$\eta_0 = 2\left(\varepsilon - \varepsilon^{1/L}\right), \quad (41)$$

where η_0 is the hunting area scale.

The updated position of the prey with respect to its previous position in the hunting area is expressed as

$$H_{\text{prey}}(t+1) = \boldsymbol{y}_{\text{prey}}(t) + \eta \left| \bar{\boldsymbol{y}}(t) - \boldsymbol{y}_{\text{prey}}(t) \right|, \quad (42)$$

$$\eta = \eta_0 \sin(2\pi r_3), \quad (43)$$

where η is the scale of the hunting area and r_3 is a random number within (0,1). The mathematical notation of curling behavior is given as

$$s_i(t+1) = H_{\text{prey}}(t+1) + \varpi\left(H_{\text{prey}}(t+1) - \text{round}(\text{rand})\, y_i(t)\right), \quad (44)$$

where ϖ is the curling factor and is defined as

$$\varpi = \varepsilon^{\frac{r_4(1-l)}{L}} \cos(2\pi r_4), \quad (45)$$

with r_4 being a random number within (0,1).

3.4 Migration phase

An eel migrates from the resting phase to the migration phase when it finds prey. Mathematically, this is expressed as

$$s_i(t+1) = r_5 R_i(t+1) + r_6 A_{\text{r}}(t+1) - D\left(A_{\text{r}}(t+1) - y_i(t)\right), \quad (46)$$

$$A_{\text{r}}(t+1) = \boldsymbol{y}_{\text{prey}}(t) + \eta \left| \bar{\boldsymbol{y}}(t) - \boldsymbol{y}_{\text{prey}}(t) \right|, \quad (47)$$

where A_{r} is a random position in the hunting area, and r_5 and r_6 are random numbers within (0,1). $A_{\text{r}}(t+1)-y_i(t)$ indicates the movement of prey towards the hunting area. D is the Lévy flight function, introduced for the exploitation phase of EEFOA to avoid becoming stuck in local minima.

To obtain the Lévy flight, we have

$$D = 0.001\left|\frac{v-\theta}{|\vartheta|^{1/x}}\right|, \quad (48)$$

$$v, \vartheta \sim N(0,1), \quad (49)$$

$$\theta = \left(\frac{\Gamma(1+x)\sin\left(\frac{\pi x}{2}\right)}{\Gamma\left(\frac{1+x}{2}\right) x \cdot 2^{\frac{x-1}{2}}}\right)^{1/x}, \quad (50)$$

where Γ is the gamma function and x=1.5.

An eel observes the current position of the prey by transmitting an electric signal of low electric discharge and continuously observing the prey. If the foraging process is observed, the eel moves to the candidate position or otherwise stays in position. The position of the eels is updated by

$$y_i(t+1) = \begin{cases} y_i(t), & \text{fitness}(y_i(t)) \leq \text{fitness}(s_i(t+1)), \\ s_i(t+1), & \text{fitness}(y_i(t)) > \text{fitness}(s_i(t+1)). \end{cases} \quad (51)$$

3.5 Energy factor

An energy factor dynamically controls the shift between the exploration and exploitation phases. It decreases over time, increasing the focus on exploitation as the search progresses. Mathematically, the energy factor is computed as

$$K(t) = 4\sin\left(1 - \frac{t}{L}\right)\ln\frac{1}{r_7}, \quad (52)$$

where r_7 is a random number within (0, 1). From Eq. (52), it can be seen that the energy factor K decreases with increasing number of iterations. If K>1, the global search is completed, resulting in exploration. However, when the energy factor K≤1, local search is performed, resulting in exploitation.

The computational process is expressed as

$$\sigma_K = 1 - \frac{t}{L}, \quad (53)$$

while the energy factor K is given by

$$K(t) = \sin(\sigma_K)\ln\frac{1}{r_7}. \quad (54)$$

The K's probability can be given as (Zhao WG et al., 2024)

$$P\{K(t)>1\}=\frac{\int_0^1\int_0^{\mathrm{e}^{-\frac{1}{4\sin(\sigma_K)}}}\mathrm{d}r\mathrm{d}\sigma_K}{1}=-\int_{-\infty}^{-\frac{1}{4\sin(1)}}\frac{\mathrm{e}^y\mathrm{d}y}{y\sqrt{16y^2-1}}\approx 0.5035. \tag{55}$$

According to the expression in Eq. (55), there is a 50% probability for switching between the exploration and exploitation phases during the optimization process.

3.6 Pseudo code

The pseudo code of EEFOA is presented in Algorithm 1.

4 Findings and analysis

The outcomes of simulations are discussed in this section. The input signal is a random signal with zero mean and unit variance, while the Gaussian distributed signal with zero mean and constant variance is considered to be noise. The findings include the results and corresponding analysis after extensive simulations to elaborate the effectiveness of the recently proposed EEFOA for a fractional-HARX system. The simulations are executed on Intel® Core™ i7-9700 CPU @3.00 GHz with 40 GB DDR4 RAM.

The study on fractional-HARX system with second-order nonlinearity (case study 1) is conducted to exploit the unique mechanisms of EEFOA. The system is represented by six parameters, i.e., $[k_1, k_2, j_1, j_2, r_1, r_2]$, where the fractional order is 0.4. The performance is assessed through five different noise scenarios, i.e., u=0, 0.000 15, 0.0015, 0.015, and 0.15, and multiple evaluation metrics. The tuned parameters of the proposed EEFOA are taken from Zhao WG et al. (2024). The second-order nonlinear fractional-HARX system is expressed as follows:

$$K(z)=1+0.45(z^{-1})^{0.4}+0.29(z^{-2})^{0.4}, \tag{56}$$

$$J(z)=0.16(z^{-1})^{0.4}+0.56(z^{-1})^{0.4}, \tag{57}$$

$$\bar{m}(t)=0.35m(t)+0.8(m(t))^2, \tag{58}$$

where the parameter vector is given as

Algorithm 1 Electric eel foraging optimization algorithm

Input: Features of the best solution

Output: $\boldsymbol{y}_{\text{prey}}$

Step 1: Set parameters of EEFOA

Number of individual electric eels: n

Dimension: d

Number of iterations: L

Execution of EEFOA

Step 2: Initialization

Initialize the random population: y_i (i=1, 2, ⋯, n)

Estimate fitness$_i$ and $\boldsymbol{y}_{\text{prey}}$

while

The stopping condition is not met

do

Step 3: Calculate the energy factor

for

Each individual eel y_i

do

Calculate the energy factor K using Eq. (52)

if K>1

Step 4: Interaction phase

Use Eq. (29) to evaluate fitness$_i$

else

Step 5: Resting phase

if Rand<1/3

Determine the resting phase using Eq. (36)

Eels execute resting behavior using Eq. (38)

Calculate fitness$_i$

else Rand>2/3

Step 6: Migration phase

Execute migration phase using Eq. (46)

else

Step 7: Hunting phase

Calculate the hunting region using Eq. (42)

Perform hunting using Eq. (44)

end if

end if

Update individual eel's position using Eq. (51)

end for

Update the best solution $\boldsymbol{y}_{\text{prey}}$

end while

Return $\boldsymbol{y}_{\text{prey}}$

$$\boldsymbol{\omega}=\left[\omega_1,\omega_2,\omega_3,\omega_4,\omega_5,\omega_6\right]$$
$$=\left[k_1,k_2,j_1,j_2,r_1,r_2\right]=\left[0.45,0.29,0.16,0.56,0.35,0.8\right].$$

Initially the performance of the proposed EEFOA for fractional-HARX is assessed using convergence characteristics. The simulations are executed for five noise scenarios, i.e., u=0, 0.000 15, 0.0015, 0.015, and 0.15, separately. To analyze the convergence behavior and steady-state response efficiently, different numbers of iterations are selected. The system is also analyzed with 50, 100, and 150 search agents, but no significant change is observed. This is why 50 search agents are selected for the rest of the study.

Fig. 3 presents the convergence plots of the best run over 60 independent runs for all noise scenarios. For u=0, EEFOA achieves a commendable fitness value higher than E-30, while for u=0.000 15, 0.0015, 0.015, and 0.15 the fitness values are 1.27892E-08, 1.42604E-06, 1.63598E-04, and 2.06484E-02, respectively. While EEFOA does a commendable job with the fractional-HARX system, its performance is negatively affected by increased noise.

The simulations are performed for 60 autonomous runs to examine the convergence of EEFOA for fractional-HARX. For u=0.000 15, 0.0015, 0.015, and 0.15, plots are given for 100, 200, 300, and 500 iterations. For instance, for u=0.000 15, it is observed that increasing the iteration count stabilizes the performance of EEFOA. All noise scenarios at 500 iterations provide consistent and stable fitness, as witnessed in Fig. 4. However, EEFOA becomes consistent before 500 iterations. Generally, the statistical analysis indicates that EEFOA is very consistent, stable, and robust, as it provides consistent fitness in early iterations.

EEFOA's performance is also examined in terms of its exactness and correctness in the estimation of the desired parameters of the system. The weight estimation plot for all noise levels on the best independent run is presented in Figs. 5–9. Simulation results demonstrate that increasing the noise level decreases the exactness in estimating the desired weights, as given in Table 1. For instance, for the noise-free scenario, the desired parameters are estimated exactly before 500 iterations. This depicts EEFOA's rapid parameter estimation capability and fast convergence to steady-state values. Similarly, when we increase the noise up to u=0.015, EEFOA still provides an accurate estimation of parameters to a very close value. In a very high noise scenario at level u=0.15, the accuracy is slightly disturbed, as observed in Fig. 10. Additionally, some

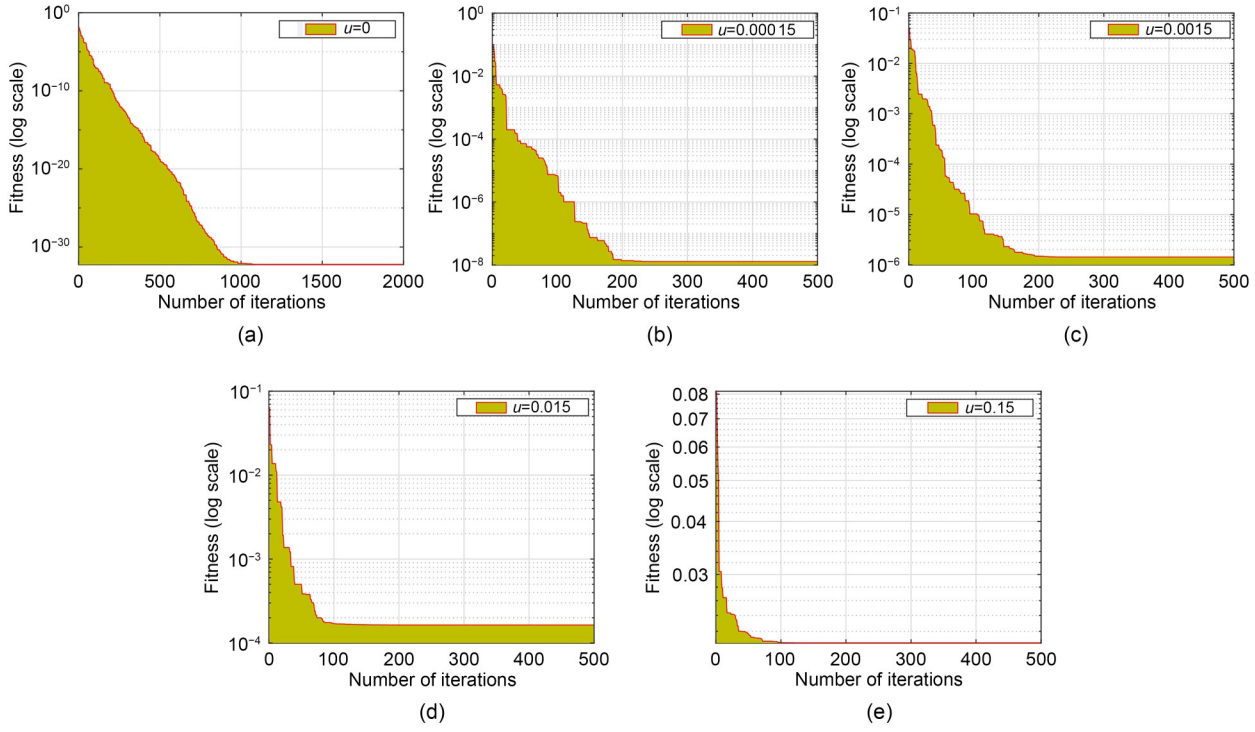

Fig. 3 Learning curves for all noise scenarios of case study 1: (a) u=0; (b) u=0.000 15; (c) u=0.0015; (d) u=0.015; (e) u=0.15

Table 1 The best estimated parameters for all noise scenarios of case study 1

Noise level	ω_1	ω_2	ω_3	ω_4	ω_5	ω_6
u=0	0.4500	0.2900	0.1600	0.5600	0.3500	0.8000
u=0.000 15	0.4497	0.2897	0.1597	0.5597	0.3500	0.8000
u=0.0015	0.4525	0.2924	0.1625	0.5617	0.3466	0.7977
u=0.015	0.4707	0.3118	0.1853	0.5659	0.3390	0.7958
u=0.15	0.3454	0.1931	0.0405	0.4621	0.7026	0.9874

fluctuations in the convergence curves are seen during the initial iterations and then become stable during the steady state. The results confirm the robustness of EEFOA in estimating the parameters of a fractional-HARX system for different noise scenarios.

To delve deeper into the performance, bar charts presenting the average accuracy are given in Fig. 10. It is observed from both Fig. 10 and Table 2 that the

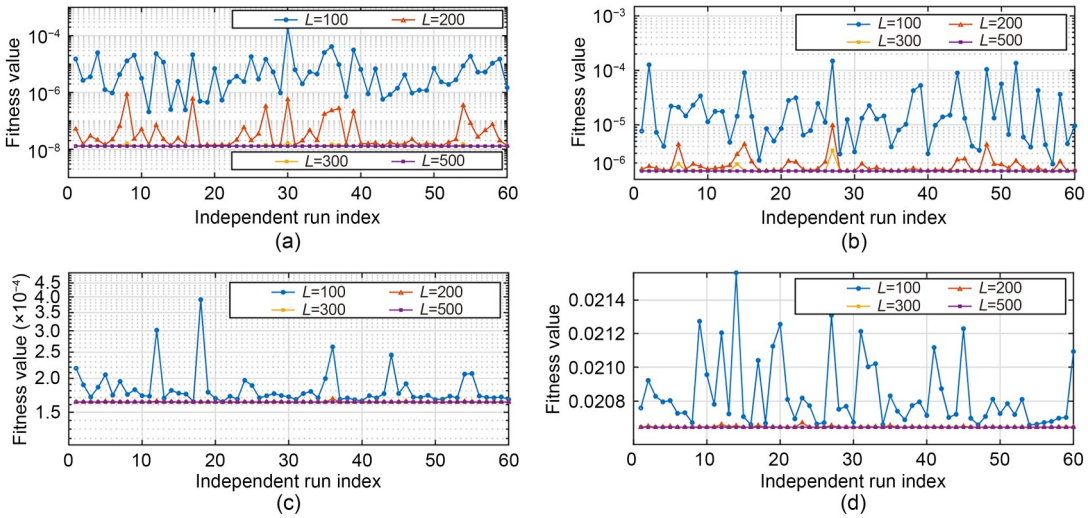

Fig. 4 Statistical plots at different iteration levels of case study 1: (a) u=0.000 15; (b) u=0.0015; (c) u=0.015; (d) u=0.15

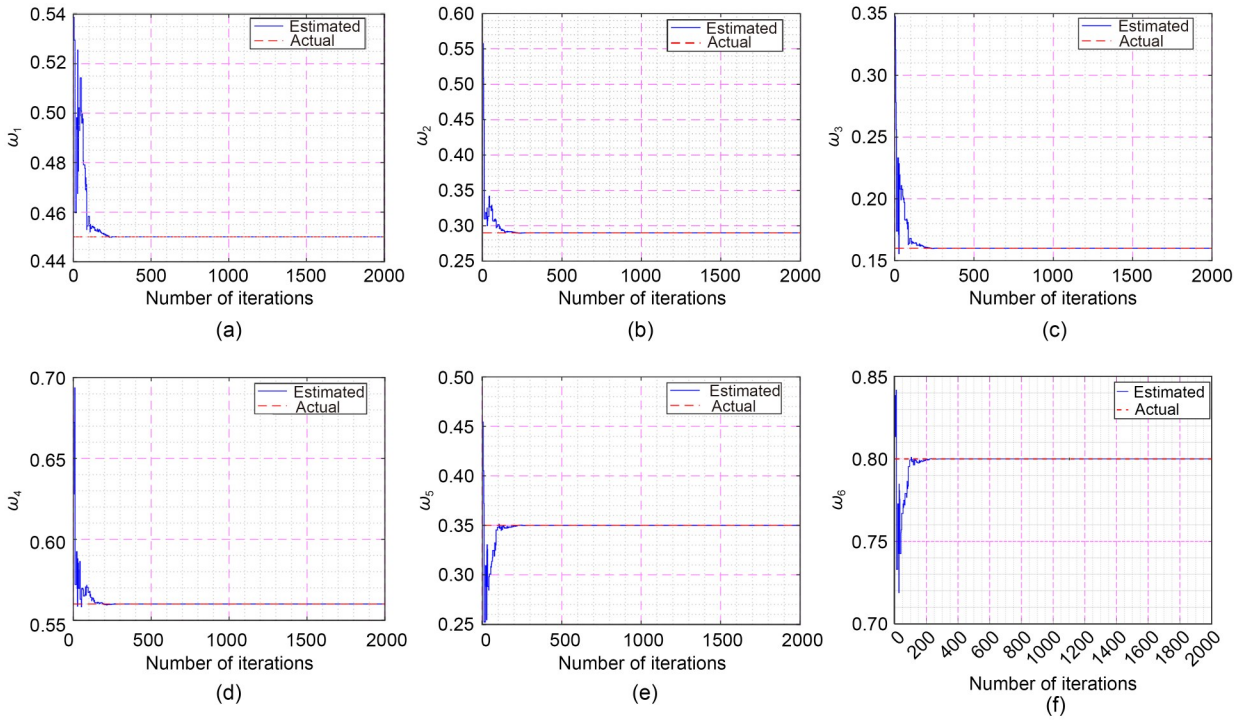

Fig. 5 Estimated parameter curves of the best independent run for u=0 in case study 1: (a) ω_1; (b) ω_2; (c) ω_3; (d) ω_4; (e) ω_5; (f) ω_6

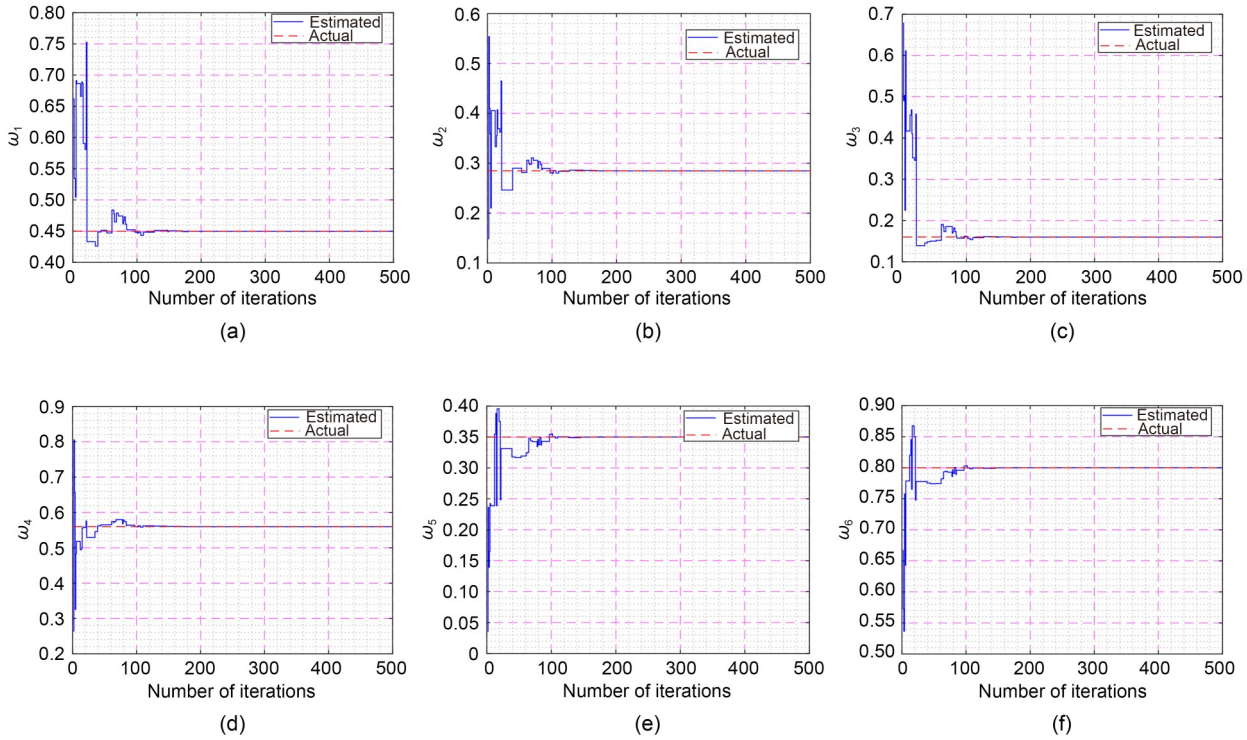

Fig. 6 Estimated parameter curves of the best independent run for u=0.000 15 in case study 1: (a) ω_1; (b) ω_2; (c) ω_3; (d) ω_4; (e) ω_5; (f) ω_6

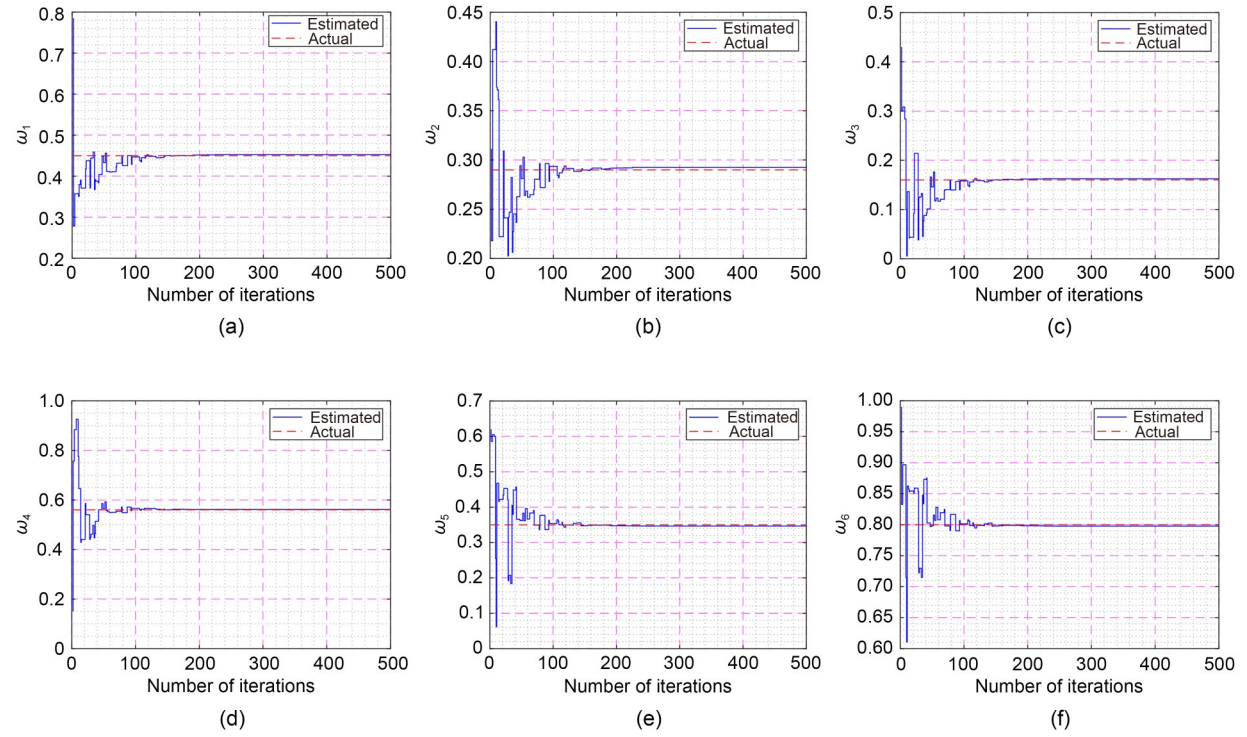

Fig. 7 Estimated parameter curves of the best independent run for u=0.0015 in case study 1: (a) ω_1; (b) ω_2; (c) ω_3; (d) ω_4; (e) ω_5; (f) ω_6

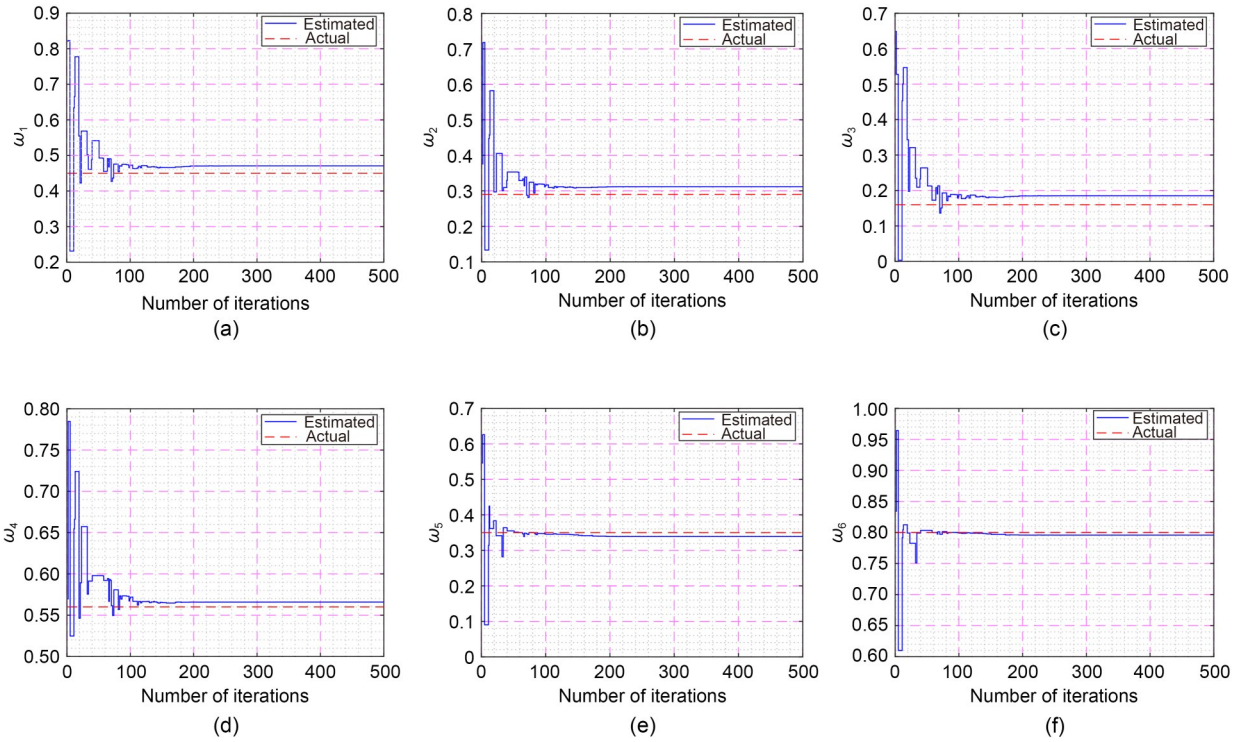

Fig. 8 Estimated parameter curves of the best independent run for u=0.015 in case study 1: (a) ω_1; (b) ω_2; (c) ω_3; (d) ω_4; (e) ω_5; (f) ω_6

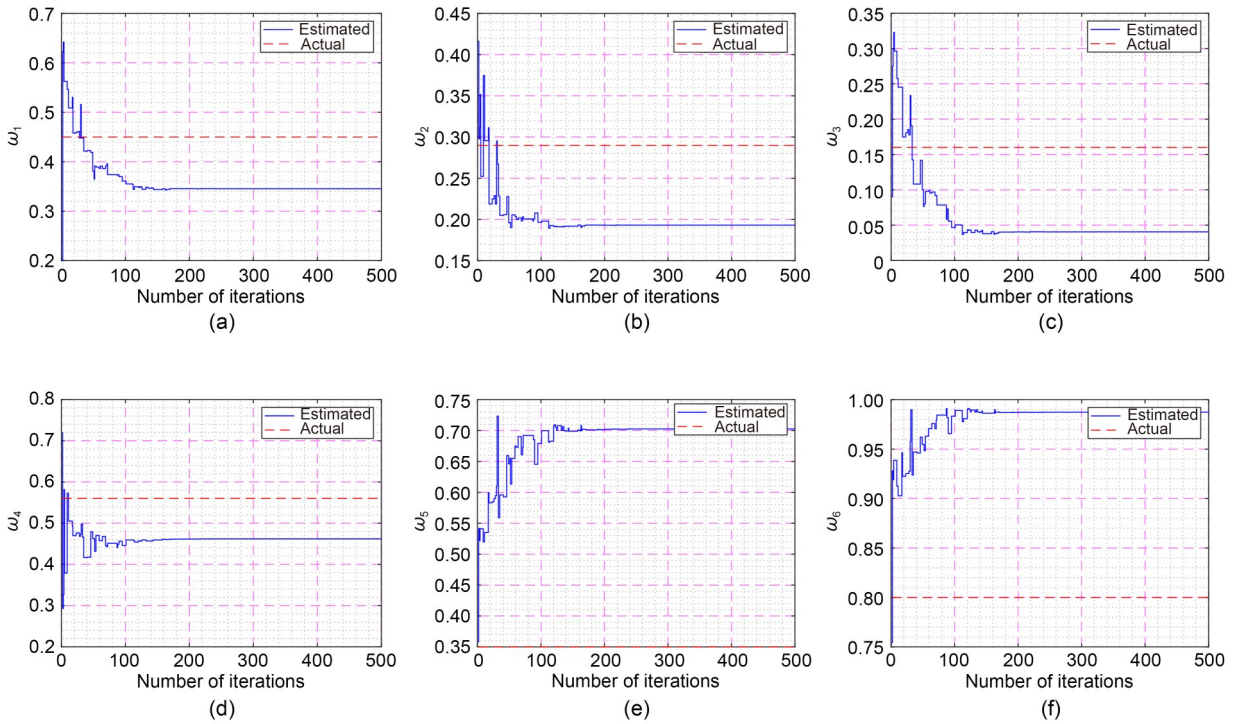

Fig. 9 Estimated parameter curves of the best independent run for u=0.15 in case study 1: (a) ω_1; (b) ω_2; (c) ω_3; (d) ω_4; (e) ω_5; (f) ω_6

best fitness is very close to the average fitness, which indicates that the EEFOA's performance is very consistent and stable. The best, average, and worst fitnesses are 1.42604E-06, 1.42606E-06, and 1.42668E-06 respectively for u=0.0015. The values are very close, indicating the competence of EEFOA in providing stable fitness over independent runs.

A further examination is based on Nash–Sutcliffe efficiency (NSE); the value of NSE ranges from $-\infty$ to 1. A higher NSE value indicates a better performance of the model, and 1 indicates the best fit. Fig. 11 presents the NSE-based learning curves for all noise levels. The investigation yields that EEFOA achieves NSE values of 1, 0.999 999, 0.999 85, and 0.993 212 for noise levels of u=0, 0.000 15, 0.0015, and 0.015, respectively. These NSE values indicate the good performance of EEFOA in the identification of desired parameters. Moreover, for a very high noise level of u=0.15, the NSE value achieved approaches zero, exhibiting the natural behavior of the system. However, the noise level of u=0.015 is also high, but EEFOA performs well up to that level of noise.

The results for case study 2 of a fractional-HARX system with third-order nonlinearity are provided in the supplementary materials.

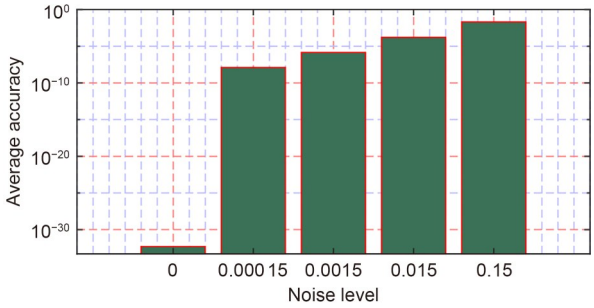

Fig. 10 Comparison of average accuracy for different noise scenarios in case study 1

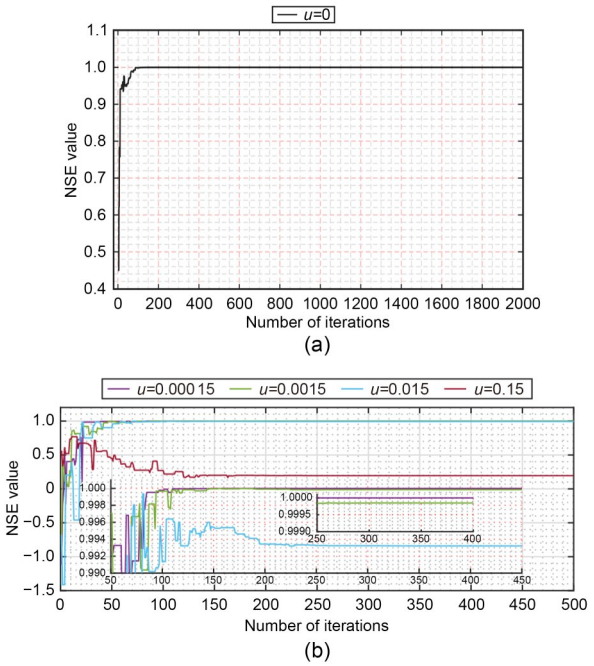

Fig. 11 NSE-based curves for all disturbance levels of case study 1: (a) noise-free scenario; (b) noisy scenario

5 Conclusions

In this study, the identification problem of fractional-HARX was addressed using the swarm intelligence-based computing of EEFOA. The key-term separation principle was incorporated to reduce the redundant parameters that occur due to cross-product terms in the system's information vector. The proposed scheme was evaluated for five different noise scenarios in two different fractional-HARX models with variation in the order of nonlinearity. The efficiency, robustness, and accuracy of the system were validated through learning curve plots, statistical analyses, and weight estimation plots. However, the plots of the NSE metric advocated the performance and stability

Table 2 Comparison: ranks of fitness, from the best to the worst, along with standard deviations for case study 1

Noise level	Best fitness	Mean fitness	Worst fitness	Standard deviation
u=0	0.00000E+00	4.96017E-33	5.39569E-32	8.90802E-33
u=0.000 15	1.27892E-08	1.27892E-08	1.27894E-08	2.82445E-14
u=0.0015	1.42604E-06	1.42606E-06	1.42668E-06	9.90498E-11
u=0.015	1.63598E-04	1.63598E-04	1.63598E-04	2.76177E-12
u=0.15	2.06484E-02	2.06484E-02	2.06485E-02	2.02044E-09

of EEFOA for the fractional-HARX model. The statistical results in terms of best, average, and worst fitness values and standard deviation for five distinct noise scenarios confirmed the efficacy of EEFOA for the parameter estimation in fractional-HARX models, even for stiff third-order nonlinear fractional-HARX. The EEFOA and AVOA achieved a fitness value of level 10^{-6}, WOA and HOA obtained a fitness value of around 10^{-4}, and RSA provided a 10^{-3} fitness value for a u= 0.0015 noise scenario. Thus, the given methodology was verified to be accurate in comparison with recent counterpart optimization algorithms as endorsed by exhaustive simulations of various scenarios. In the future, applications of the proposed computing approach can be explored in solving the battery state of charge estimation (Li ZX et al., 2023, 2024) and hydropower generation problems (Zhao ZW et al., 2022; Wang PF et al., 2023a, 2023b).

Contributors

Muhammad Asif Zahoor RAJA and Naveed Ishtiaq CHAUDHARY designed the research. Ching-Lung CHANG supervised the research. Chi-Min SHU provided the resources and administered the project. Faisal ALTAF and Taimoor Ali KHAN drafted the paper. Naveed Ishtiaq CHAUDHARY and Zeshan Aslam KHAN revised and finalized the paper.

Conflict of interest

All the authors declare that they have no conflict of interest.

Data availability

The data that support the findings of this study are available from the corresponding author upon reasonable request.

References

Abdollahzadeh B, Gharehchopogh FS, Mirjalili S, 2021. African vultures optimization algorithm: a new nature-inspired metaheuristic algorithm for global optimization problems. *Comput Ind Eng*, 158:107408. https://doi.org/10.1016/j.cie.2021.107408

Abdollahzadeh B, Khodadadi N, Barshandeh S, et al., 2024. Puma optimizer (PO): a novel metaheuristic optimization algorithm and its application in machine learning. *Cluster Comput*, 27(4):5235-5283. https://doi.org/10.1007/s10586-023-04221-5

Abualigah L, Abd Elaziz M, Sumari P, et al., 2022. Reptile search algorithm (RSA): a nature-inspired meta-heuristic optimizer. *Expert Syst Appl*, 191:116158. https://doi.org/10.1016/j.eswa.2021.116158

Ala A, Goli A, Mirjalili S, et al., 2024. A fuzzy multi-objective optimization model for sustainable healthcare supply chain network design. *Appl Soft Comput*, 150:111012. https://doi.org/10.1016/j.asoc.2023.111012

Ali R, Asjad MI, Akgül A, 2021. An analysis of a mathematical fractional model of hybrid viscous nanofluids and its application in heat and mass transfer. *J Comput Appl Math*, 383:113096. https://doi.org/10.1016/j.cam.2020.113096

Altaf F, Chang CL, Chaudhary NI, et al., 2025. Astrophysical expedition: transit search heuristics for fractional Hammerstein control autoregressive models. *Mod Phys Lett B*, 39(7):2450417. https://doi.org/10.1142/S0217984924504177

Dong RY, Sun LX, Ma L, et al., 2023. Boosting kernel search optimizer with slime mould foraging behavior for combined economic emission dispatch problems. *J Bionic Eng*, 20(6):2863-2895. https://doi.org/10.1007/s42235-023-00408-z

El-Hasnony IM, Barakat SI, Mostafa RR, 2020. Optimized ANFIS model using hybrid metaheuristic algorithms for Parkinson's disease prediction in IoT environment. *IEEE Access*, 8:119252-119270. https://doi.org/10.1109/ACCESS.2020.3005614

Fang LL, Liang XY, 2023. A novel method based on nonlinear binary grasshopper whale optimization algorithm for feature selection. *J Bionic Eng*, 20(1):237-252. https://doi.org/10.1007/s42235-022-00253-6

Frikh ML, Boutasseta N, 2024. Pitch angle control of wind turbines using model-free auto-tuned fractional order proportional derivative ATFOPD controller. *Comput Electr Eng*, 116:109199. https://doi.org/10.1016/j.compeleceng.2024.109199

Gamini S, Kumar SS, 2023. Homomorphic filtering for the image enhancement based on fractional-order derivative and genetic algorithm. *Comput Electr Eng*, 106:108566. https://doi.org/10.1016/j.compeleceng.2022.108566

González-Patiño D, Villuendas-Rey Y, Argüelles-Cruz AJ, et al., 2019. A novel bio-inspired method for early diagnosis of breast cancer through mammographic image analysis. *Appl Sci*, 9(21):4492. https://doi.org/10.3390/app9214492

Han Y, Chen WB, Heidari AA, et al., 2023. Multi-verse optimizer with Rosenbrock and diffusion mechanisms for multilevel threshold image segmentation from COVID-19 chest X-ray images. *J Bionic Eng*, 20(3):1198-1262. https://doi.org/10.1007/s42235-022-00295-w

Heidari AA, Mirjalili S, Faris H, et al., 2019. Harris hawks optimization: algorithm and applications. *Fut Gener Comput Syst*, 97:849-872. https://doi.org/10.1016/j.future.2019.02.028

Hu HY, Xie ZK, Wang DQ, 2024. Temporal pattern attention based Hammerstein model for estimating battery SOC. *J Energy Storage*, 100:113666. https://doi.org/10.1016/j.est.2024.113666

Ionescu C, Lopes A, Copot D, et al., 2017. The role of fractional calculus in modeling biological phenomena: a review. *Commun Nonl Sci Numer Simul*, 51:141-159. https://doi.org/10.1016/j.cnsns.2017.04.001

Jakšić Z, Devi S, Jakšić O, et al., 2023. A comprehensive review of bio-inspired optimization algorithms including applications

in microelectronics and nanophotonics. *Biomimetics*, 8(3):278. https://doi.org/10.3390/biomimetics8030278

Karaca Y, 2023. Fractional calculus operators–Bloch–Torrey partial differential equation–artificial neural networks–computational complexity modeling of the micro–macrostructural brain tissues with diffusion MRI signal processing and neuronal multi-components. *Fractals*, 31(10): 2340204. https://doi.org/10.1142/S0218348X23402041

Kausar A, Chang CY, Raja MAZ, et al., 2025. A novel design of layered recurrent neural networks for fractional order Caputo–Fabrizio stiff electric circuit models. *Mod Phys Lett B*, 39(2):2450393. https://doi.org/10.1142/S0217984924503937

Khan TA, Chaudhary NI, Khan ZA, et al., 2024a. Design of Runge–Kutta optimization for fractional input nonlinear autoregressive exogenous system identification with key-term separation. *Chaos Sol Fract*, 182:114723. https://doi.org/10.1016/j.chaos.2024.114723

Khan TA, Chaudhary NI, Hsu CC, et al., 2024b. A gazelle optimization expedition for key term separated fractional nonlinear systems with application to electrically stimulated muscle modeling. *Chaos Sol Fract*, 185:115111. https://doi.org/10.1016/j.chaos.2024.115111

Li F, Liang MJ, Luo YS, 2023a. Correlation analysis-based parameter learning of Hammerstein nonlinear systems with output noise. *Eur J Contr*, 72:100819. https://doi.org/10.1016/j.ejcon.2023.100819

Li F, Zheng T, Cao QF, 2023b. Modeling and identification for practical nonlinear process using neural fuzzy network–based Hammerstein system. *Trans Inst Meas Contr*, 45(11): 2091-2102. https://doi.org/10.1177/01423312221143777

Li F, Zhu XJ, Cao QF, 2023c. Parameter learning for the nonlinear system described by a class of Hammerstein models. *Circ Syst Signal Process*, 42(5):2635-2653. https://doi.org/10.1007/s00034-022-02240-y

Li F, Zhou SB, Liu RR, 2024. Parameter estimation for the Hammerstein–Wiener nonlinear system and application in lithium-ion batteries. *J Energy Storage*, 102:114265. https://doi.org/10.1016/j.est.2024.114265

Li S, Huang CD, Song XS, 2023. Novel method to detect Hopf bifurcation in a delayed fractional-order network model with bidirectional ring structure. *Int J Biomath*, 16(6):2250117. https://doi.org/10.1142/S1793524522501170

Li ZQ, Wang WW, Zhang CL, et al., 2023. Fault-tolerant control based on fractional sliding mode: crawler plant protection robot. *Comput Electr Eng*, 105:108527. https://doi.org/10.1016/j.compeleceng.2022.108527

Li ZX, Yang Y, Li LW, et al., 2023. A weighted Pearson correlation coefficient based multi-fault comprehensive diagnosis for battery circuits. *J Energy Storage*, 60:106584. https://doi.org/10.1016/j.est.2022.106584

Li ZX, Li LW, Chen J, et al., 2024. A multi-head attention mechanism aided hybrid network for identifying batteries' state of charge. *Energy*, 286:129504. https://doi.org/10.1016/j.energy.2023.129504

Liu X, Wang C, Dai W, 2024. Probability-based identification of Hammerstein systems with asymmetric noise characteristics. *IEEE Trans Instrum Meas*, 73:6500611. https://doi.org/10.1109/TIM.2023.3336437

Machado JAT, Lopes AM, 2015. Analysis of natural and artificial phenomena using signal processing and fractional calculus. *Fract Calc Appl Anal*, 18(2):459-478. https://doi.org/10.1515/fca-2015-0029

Malik MF, Chang CL, Aslam MS, et al., 2022. Fuzzy-evolution computing paradigm for fractional Hammerstein control autoregressive systems. *Int J Fuzzy Syst*, 24(5):2447-2475. https://doi.org/10.1007/s40815-022-01291-2

Malik MF, Chang CL, Chaudhary NI, et al., 2023. Swarming intelligence heuristics for fractional nonlinear autoregressive exogenous noise systems. *Chaos Sol Fract*, 167:113085. https://doi.org/10.1016/j.chaos.2022.113085

Malik NA, Chang CL, Chaudhary NI, et al., 2024. Astrophysics-based transit search optimization heuristics for parameter estimation of multi-frequency sinusoidal signals. *Mod Phys Lett B*, 38(34):2450342. https://doi.org/10.1142/S0217984924503421

Mathi MT, Baburaj E, 2022. Comparative analysis of bio-inspired optimization algorithms in neural network-based data mining classification. *Int J Swarm Intell Res*, 13(1):25. https://doi.org/10.4018/IJSIR.2022010103

Megherbi O, Hamiche H, Bettayeb M, 2024. Implementation of a wireless text data transmission based on the impulsive control of fractional-order chaotic systems. *Comput Electr Eng*, 116:109224. https://doi.org/10.1016/j.compeleceng.2024.109224

Mehmood K, Chaudhary NI, Khan ZA, et al., 2024. Atomic physics-inspired atom search optimization heuristics integrated with chaotic maps for identification of electro-hydraulic actuator systems. *Mod Phys Lett B*, 38(30): 2450308. https://doi.org/10.1142/S0217984924503081

Mehmood N, Abbas A, Akgül A, et al., 2023. Existence and stability results for coupled system of fractional differential equations involving AB-Caputo derivative. *Fractals*, 31(2):2340023. https://doi.org/10.1142/S0218348X23400236

Mirjalili S, Lewis A, 2016. The whale optimization algorithm. *Adv Eng Softw*, 95:51-67. https://doi.org/10.1016/j.advengsoft.2016.01.008

Mukhtar R, Chang CY, Raja MAZ, et al., 2024. Novel nonlinear fractional order Parkinson's disease model for brain electrical activity rhythms: intelligent adaptive Bayesian networks. *Chaos Sol Fract*, 180:114557. https://doi.org/10.1016/j.chaos.2024.114557

Padhi JR, Deeb MA, Tripathy S, et al., 2023. Fractional calculus based PI-FOPID controller for frequency deviation control in integrated power system. Proc Electric Power and Renewable Energy Conf, p.213-224.

Partohaghighi M, Yusuf A, Alshomrani AS, et al., 2024. Fractional hyper-chaotic system with complex dynamics and high sensitivity: applications in engineering. *Int J Mod Phys B*, 38(1):2450012. https://doi.org/10.1142/S0217979224500127

Rahmanshahi M, Jafari-Asl J, Fathi-Moghadam M, et al., 2024. Metaheuristic learning algorithms for accurate prediction of hydraulic performance of porous embankment weirs. *Appl Soft Comput*, 151:111150. https://doi.org/10.1016/j.asoc.2023.111150

Šapina M, Garcin M, Kramarić K, et al., 2020. The Hurst exponent of heart rate variability in neonatal stress, based on a mean-reverting fractional Lévy stable motion. *Fluctuat Noise Lett*, 19(3):2050026. https://doi.org/10.1142/S0219477520500261

Sowa M, Majka Ł, Wajda K, 2023. Excitation system voltage regulator modeling with the use of fractional calculus. *AEU-Int J Electron Commun*, 159:154471. https://doi.org/10.1016/j.aeue.2022.154471

Sweis H, Arqub OA, Shawagfeh N, 2023. Fractional delay integrodifferential equations of nonsingular kernels: existence, uniqueness, and numerical solutions using Galerkin algorithm based on shifted Legendre polynomials. *Int J Mod Phys C*, 34(4):2350052. https://doi.org/10.1142/S0129183123500523

Tubishat M, Al-Obeidat F, Sadiq AS, et al., 2023. An improved dandelion optimizer algorithm for spam detection: next-generation email filtering system. *Computers*, 12(10):196. https://doi.org/10.3390/computers12100196

Vyawahare VA, Nataraj PSV, 2013. Fractional-order modeling of neutron transport in a nuclear reactor. *Appl Math Modell*, 37(23):9747-9767. https://doi.org/10.1016/j.apm.2013.05.023

Wang DQ, 2024. Key-term separation based hierarchical gradient approach for NN based Hammerstein battery model. *Appl Math Lett*, 157:109207. https://doi.org/10.1016/j.aml.2024.109207

Wang PF, Xu ZK, Chen DY, 2023a. An integrated framework for reliability prediction and condition-based maintenance policy for a hydropower generation unit using GPHM and SMDP. *Reliab Eng Syst Saf*, 238:109419. https://doi.org/10.1016/j.ress.2023.109419

Wang PF, Guo YX, Xu ZK, et al., 2023b. A novel approach of full state tendency measurement for complex systems based on information causality and PageRank: a case study of a hydropower generation system. *Mech Syst Signal Process*, 187:109956. https://doi.org/10.1016/j.ymssp.2022.109956

Wang SW, Xiao XP, Ding Q, 2024. A novel fractional system grey prediction model with dynamic delay effect for evaluating the state of health of lithium battery. *Energy*, 290:130057. https://doi.org/10.1016/j.energy.2023.130057

Ye SQ, Zhou KQ, Zain AM, et al., 2023. A modified harmony search algorithm and its applications in weighted fuzzy production rule extraction. *Front Inform Technol Electron Eng*, 24(11):1574-1590. https://doi.org/10.1631/FITEE.2200334

Zhang MG, Li F, Yu Y, et al., 2024. Estimation of Hammerstein nonlinear systems with noises using filtering and recursive approaches for industrial control. *Front Inform Technol Electron Eng*, 25(2):260-271. https://doi.org/10.1631/FITEE.2300620

Zhang XF, Boutat D, Liu DY, 2023. Applications of fractional operator in image processing and stability of control systems. *Fract Fract*, 7(5):359. https://doi.org/10.3390/fractalfract7050359

Zhao WG, Wang LY, Zhang ZX, et al., 2024. Electric eel foraging optimization: a new bio-inspired optimizer for engineering applications. *Expert Syst Appl*, 238:122200. https://doi.org/10.1016/j.eswa.2023.122200

Zhao ZW, Yuan YC, He MJ, et al., 2022. Stability and efficiency performance of pumped hydro energy storage system for higher flexibility. *Renew Energy*, 199:1482-1494. https://doi.org/10.1016/j.renene.2022.09.085

List of supplementary materials

1 Extension of case study 2 of a fractional-HARX system with third-order nonlinearity

Table S1 Estimated parameters for all noise scenarios of case study 2

Table S2 Comparison: ranks of fitness, from the best to the worst, along with standard deviations for case study 2

Table S3 EEFOA's computational complexity analysis

Fig. S1 Case study 2: iterative fitness curves of the best independent execution for all noise scenarios

Fig. S2 Case study 2: statistical analysis over 60 independent runs

Fig. S3 Case study 2: parameter estimation curves for the best independent run for u=0

Fig. S4 Case study 2: parameter estimation curves for the best independent run for u=0.000 15

Fig. S5 Case study 2: parameter estimation curves for the best independent run for u=0.0015

Fig. S6 Case study 2: parameter estimation curves for the best independent run for u=0.015

Fig. S7 Case study 2: parameter estimation curves for the best independent run for u=0.15

Fig. S8 Average accuracy bar chart for all disturbance variations of case study 2

Fig. S9 NSE-based convergence curves for case study 2

Fig. S10 NSE-based statistical analysis over 60 independent runs of case study 2

Fig. S11 Comparison between EEFOA and recent equivalent algorithms for case study 2